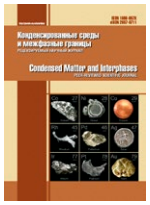

ISSN 1606-867X (Print)
ISSN 2687-0711 (Online)
Конденсированные среды и межфазные границы
https://journals.vsu.ru/kcmf/

Оригинальные статьи

Научная статья
https://doi.org/10.17308/kcmf.2025.27/13254

Structural, optical and magnetic properties of $CoFe_{2-x}Eu_xO_4$ nanoparticles prepared by simple co-precipitation route

Le Ngoc Khanh Nhu[1], Nguyen Thi Thu Trang[1], Nguyen Hoang Huy[1], Tran Dinh Trinh[2], Ngoc Anh Vu Thi[3,4], Nguyen Anh Tien[1]✉

[1]Faculty of Chemistry, Ho Chi Minh City University of Education, No. 280 An Duong Vuong st., Ho Chi Minh City 700000, Vietnam

[2]VNU Key Laboratory of Advanced Materials for Green Growth, University of Science, Vietnam National University, No. 19 Le Thanh Tong st., Hoan Kiem, Hanoi 120000, Viet Nam

[3]Laboratory of Advanced Materials Chemistry, Institute for Advanced Study in Technology, Ton Duc Thang University, Ho Chi Minh City, Vietnam

[4]Faculty of Applied Sciences, Ton Duc Thang University, Ho Chi Minh City, Vietnam

Abstract

Objectives: Nanoparticles of $CoFe_{2-x}Eu_xO_4$ (x = 0, 0.025, 0.05, 0.075, and 0.1) were successfully synthesized by simple co-precipitation method.

Experimental: Field emission scanning electron microscopy (FE-SEM) images revealed europium-doped cobalt spinel ferrite nanoparticles formed after calcination of the precursor at 900 °C for 1 h, with sizes of approximately 20–40 nm. Energy dispersive X-ray spectra (EDXS) confirmed the presence of Co, Fe, Eu, and O elements with no evident of impurities. Results calculated from powder X-ray diffraction (PXRD) data show that the average crystallite size and lattice parameters decrease with increasing europium content.

Conclusions: The doping of Eu^{3+} ions in the cobalt ferrite structure affects the optical and magnetic properties of the substrate material. In this case, the values of band gap energy (E_g), coercivity (H_c) and remanent magnetization (M_r) increase with increasing concentration of Eu^{3+} ion, while optical absorption and saturation magnetization exhibit an opposite trend. The excellent optical and magnetic properties of un-doped and Eu-doped $CoFe_2O_4$ nanoparticles suggest great potential for applications related to optics and magnetism.

Keywords: Co-spinel, nanoparticles, Eu-doping, Co-precipitation, Optical property, Magnetic parameters

For citation: Le N. K. N., Nguyen T. T. T., Nguyen H. H., Tran D. T., Vu T. N. A., Nguyen A. T. Structural, optical and magnetic properties of $CoFe_{2-x}Eu_xO_4$ nanoparticles prepared by simple co-precipitation route. *Condensed Matter and Interphases*. 2025;27(4): 555–564. https://doi.org/10.17308/kcmf.2025.27/13254

✉ Nguyen Anh Tien, e-mail: tienna@hcmue.edu.vn

1. Introduction

Among inorganic oxides with small particle sizes, spinel ferrite-type RFe_2O_4 (where R is 3*d* transition metals such as Mn, Cr, Fe, Co, Ni, Zn) has attracted research attention due to its unique electrical, optical and magnetic properties [1–3]. The application fields of spinel ferrite RFe_2O_4 nanomaterials are also very abundant and diverse such as biochemical sensors, memory devices, computer components, high-density magnetic recording materials, transformer cores, permanent magnets, microwave absorbing materials [1–4]. In addition, spinel ferrites are also used for the removal of toxic organic substances in environmental treatment such as catalytic and photocatalytic decomposition of dyes, phenol, or nitrophenol [5], adsorption of congo red [6]. Among spinel ferrites, cobalt ferrite ($CoFe_2O_4$) is the of particular interest to many researchers due to its interesting physicochemical properties such as chemical and mechanical stability, high crystalline anisotropy ($K{\cdot}10^{-3} = 6.04$ emu·g^{-1}·Oe) [7], moderate saturation magnetization (M_s = 67.37 emu·g^{-1}) [8], high coercivity (H_c = 848.32 Oe) [9], ferromagnetism with high Curie temperature (T_c = 790 K) [10, 11].

Besides interesting magnetic properties, $CoFe_2O_4$ nanoparticles have recently been studied as catalytic materials and Fenton photocatalysts for various reactions due to their strong absorption of light in the ultraviolet and visible regions [8, 11–15]. It can be seen that, depending on the research objectives, there will be different adjustments to the optical and magnetic properties of spinel ferrite. This can be done through different synthesis conditions or doping with different metals on the spinel ferrite MFe_2O_4 substrate [10, 11, 16–20]. Among these approaches, doping with rare earth metal ions to modify the structural, optical and magnetic properties of cobalt ferrite has been explored. Indeed, studies by Alves [11] and Patankar [18] showed that increasing the Y^{3+} ion content in cobalt ferrite $CoFe_{2-x}Y_xO_4$ increases the coercivity and band gap values, but decreases the saturation magnetization and remanence. Vibrating sample magnetometry studies at room temperature showed that $CoFe_{1.8}Tb_{0.2}O_4$ and $CoFe_{1.8}Er_{0.2}O_4$ nanoparticles had saturation magnetizations of 60 and 80 emu·g^{-1} [19]. Gd^{3+} ion doping in cobalt ferrite reduced all three magnetic parameters of cobalt ferrite (M_s = 87.56–52.01 emu·g^{-1}, M_r = 21.2–3.40 emu·g^{-1}, and H_c = 575–50 Oe) reported in the study of Zhao et al. [20]. Using the citric sol-gel method [21], Boddolla and Ravinder successfully synthesized $CoFe_{1-x}Eu_xO_4$ nanoparticles (x = 0 and 0.1) after drying the precursor at 100 °C in 8 h and heating the dry gel at 500 °C in 4 h. However, the research of Boddolla and Ravinder only mentioned the structural characteristics of $CoFe_{1-x}Eu_xO_4$ nanocrystals synthesized using powder X-ray diffraction analysis (PXRD) and fourier-transform infrared spectra (FTIR) [21]. The optical and magnetic properties of $CoFe_{2-x}Eu_xO_4$ nanoparticles were not reported.

Un-doped and R-doped $CoFe_2O_4$ nanomaterials were mainly synthesized by wet chemical methods such as sol-gel using citric acid [3, 4,1 2], sol-gel with the assistance of polyethylene glycol [8], combustion synthesis using urea fuel (CON_2H_4) [11, 15, 22], combustion using glycine [14], hydrothermal [6, 20], or co-precipitation at room temperature [7, 13, 19, 23], co-precipitation using oleic acid [10]. In general, each synthesis method has its strengths and weaknesses. Therefore, the choice of experimental conditions depends on the specific objectives of the research. In our previous studies [9, 24–26], oxide nanoparticles with spinel structure MFe_2O_4 (M = Co, Ni) and perovskite $RFeO_3$ (R = Eu, Dy) have been successfully synthesized by co-precipitation method through hydrolysis of R^{3+} and Fe^{3+} ations at high temperature, then cooling to room temperature before adding a suitable precipitating agent. To the best of our knowledge, this simple co-precipitation route has not been reported in the literature for the study of europium-substituted cobalt spinel ferrite.

Therefore, the aim of this study was to synthesize $CoFe_{2-x}Eu_xO_4$ spinel nanoparticles (x = 0, 0.025, 0.05, 0.075, and 0.1) by simple co-precipitation method (without any gelling agent), followed by comprehensive analysis of their crystalline structures, chemical compositions, morphologies, particle sizes, optical and magnetic properties. In addition, the study also evaluated the effect of Eu^{3+} doping ion content on the structural, optical and magnetic parameters of the synthesized $CoFe_{2-x}Eu_xO_4$ nanoparticles. In this study, the doping ratio limit is chosen to be x = 0.1 [20, 21]. Due to the significant difference

in ionic radii between Fe^{3+} (r = 0.645 Å) and rare earth metal ions R^{3+} (r ~ 1.00 Å) [27], secondary crystal phases, such as perovskite $YFeO_3$ in $Co(Ni)Fe_{2-x}Y_xO_4$ spinel [18, 28], often appear when x > 0.1.

2. Experimental methods

$CoFe_{2-x}Eu_xO_4$ nanoparticles were synthesized by simple co-precipitation method according to the diagram shown in Fig. 1 [9, 24–26]. 50 mL of aqueous solution of $Co(NO_3)_2 \cdot 6H_2O$ (99.9 % purity, Thermo Scientific), $Fe(NO_3)_3 \cdot 9H_2O$ (99.9 % purity, Sigma-Aldrich), and $Eu(NO_3)_3 \cdot 6H_2O$ (99.9 % purity, Thermo Scientific) with the stoichiometric ratio of $Co^{2+} : Fe^{3+} : Eu^{3+} = 1 : (2- x) : x$ (x = 0, 0.025, 0.05, 0.075, and 0.1 in theory) was added dropwise into a beaker containing 450 mL of boiling water on a heated magnetic stirrer (t ~ 95 °C). The reaction system was maintained at 95 °C for about 10 minutes to completely hydrolyze the metal cations, then cooled to room temperature (~ 27 °C).

Next, 5% NaOH solution was added dropwise to the reaction mixture until pH value = 10 while continuously stirring [7, 19, 25]. NaOH solution was used instead of NH_3 because cobalt(II) hydroxide can be dissolved in excess ammonia as shown in equation (1), which leads to difficulty in controlling the composition of the precipitate after the reaction [27]:

$$[Co(OH)_2(H_2O)_4]_{(s)} + 6NH_{3(aq)} \rightarrow \rightarrow [Co(NH_3)_6]^{2+}_{(aq)} + 4H_2O_{(l)} + 2OH^-_{(aq)} \quad (1)$$

The precipitate was stirred for another 30 minutes, then filtered and washed with distilled water until neutral pH. Next, the obtained precipitate was air–dried at room temperature to constant weight (approximately 5 days), then ground into fine dark brown powder, serving as the precursor. $CoFe_{2-x}Eu_xO_4$ ($x \leqslant 0.1$) nanoparticles were obtained after calcining the precursor in the air, at 900 °C for 1 h. This temperature was selected based on previous research [8, 9, 15, 23], in which the obtained ferrite spinels are single-phase, have good crystallinity and reach nanometer size. The expected reaction to form ferrites $CoFe_{2-x}Eu_xO_4$ from the corresponding precipitate mixture can be described by the following equation (2):

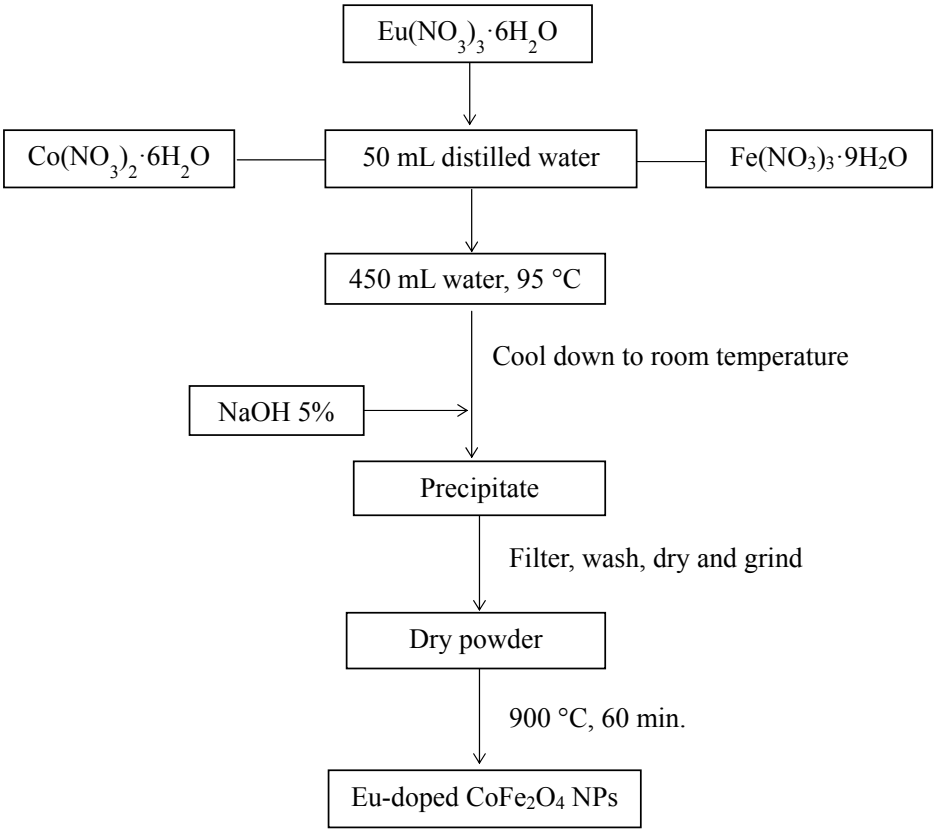

Fig. 1. Flow chart for synthesis of $CoFe_{2-x}Eu_xO_4$ nanoparticles. The synthesized samples were characterized by different methods presented in Table 1

Table 1. Analytical methods and corresponding used equipment

Analytical methods	Equipment	Experimental conditions
Powder X-ray diffraction (PXRD)	EMPYREAN X-ray diffractometer (PANanalytical, Netherlands)	– Cu*K*α radiation (λ = 1.54060 Å) – Angle range 2θ = 10–80 ° – Scanning step 0.02 °/s
Energy-dispersive X-ray spectroscopy (EDX) and EDX-mapping	FESEM S-4800 spectrometer (Hitachi, Japan)	Equipped with an EDX H-7593 (Horiba, UK)
Field emission scanning electron microscopy (FE-SEM)	FESEM S-4800 (Hitachi, Japan)	
Ultraviolet-Visible (UV-Vis) spectroscopy	Spectrophotometer UV-2600 (Shimadzu, Japan)	– Equipped with an integrating sphere (ISR-2600 Plus) – Using deuterium and halogen lamps – Using $BaSO_4$ powder as a baseline material
Vibrating-sample magnetometry (VSM)	Magnetometer MICROSENE EV11 (Japan)	– Magnetic field ranging from – 15 000 Oe to + 15 000 Oe – At room temperature

$$Co(OH)_2 + (2-x)Fe(OH)_3 + xEu(OH)_3 \rightarrow \rightarrow CoFe_{2-x}Eu_xO_4 + 4H_2O \quad (2)$$

3. Results and discussion

Fig. 2 shows the PXRD patterns of the synthesized $CoFe_{2-x}Eu_xO_4$ nanoparticles with different doping amounts of Eu^{3+} ions. All the diffraction peaks can be indexed to the cubic spinel structure of cobalt ferrite (JCPDS > 090–3471, *Fd3m space group*) and no impurity phases are observed. The PXRD pattern exhibits 9 peaks at 2θ ~ 18.30°, 30.14°, 35.52°, 37.10°, 43.14°, 53.50°, 57.04°, 62.62°, 72.40° corresponding to the Miller indices (hkl): (111), (220), (311), (222), (400), (422), (511), (440), and (533) [23]. The PXRD patterns all have flat and smooth baselines, and the obtained peaks have high intensity, proving that the synthesized $CoFe_{2-x}Eu_xO_4$ samples have good crystallinity.

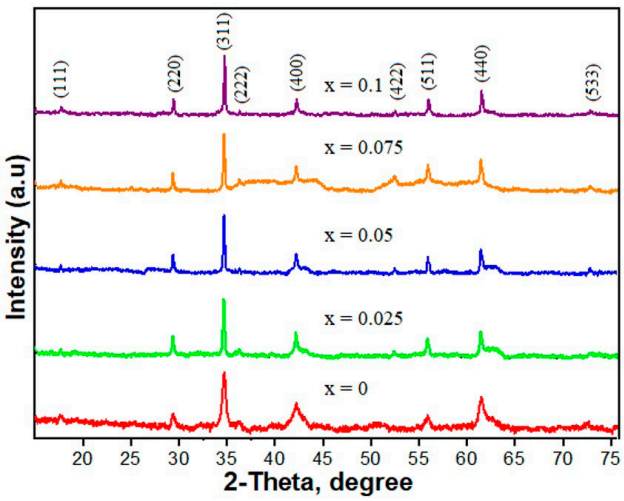

Fig. 2. PXRD patterns of Eu–doped $CoFe_2O_4$ samples annealed at 900 °C

Due to the replacement of Fe^{3+} ion by Eu^{3+} ion with larger radius ($r(Fe^{3+})$ = 0.645 Å, $r(Eu^{3+})$ = 0.950 Å), the 2θ angle is slightly shifted to the right (towards the larger angle), and a slight broadening of the peak when x increases from 0.025 to 0.1 (Fig. 3). These changes imply a decrease in the crystallite size ($D_{(hkl)}$) and the lattice parameter (*a*) of the $CoFe_{2-x}Eu_xO_4$ samples according to the following equations (3) and (4) [23, 28]:

$$D_{hkl} = \frac{k \cdot \lambda}{\beta_{hkl} \cdot \cos\theta}, \quad (3)$$

where β_{hkl} is the full-width at half maximum (FWHM, radian), θ is the corresponding diffraction angle of the maximum reflection (degree), and *k* is the shape factor (k = 0.89).

$$a = d_{hkl}\sqrt{(h^2 + k^2 + l^2)}. \quad (4)$$

Where *d* is the value of *d*-spacing of the planes and (*hkl*) are the corresponding Miller indices of the Planes.

The calculated values from PXRD patterns are listed in Table 2. It is obvious that the average crystallite sizes (*D*) and the lattice parameters (*a*, *V*) of the synthesized $CoFe_{2-x}Eu_xO_4$ samples

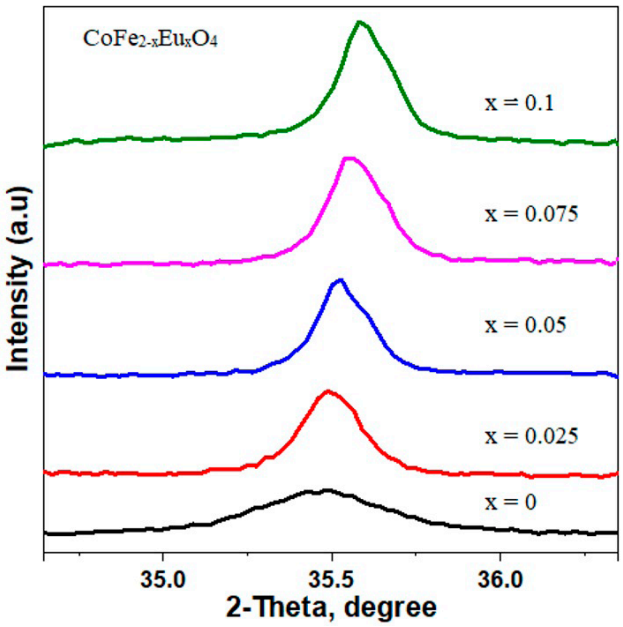

Fig. 3. PXRD patterns of peak (311) of Eu-doped $CoFe_2O_4$ samples annealed at 2θ = 34.7–36.3°

decrease with increasing the doping amount of Eu^{3+} ions. The Eu^{3+} ions, with larger radius (r = 0.950 Å), preferentially occupy octahedral positions and partially replace the Fe^{3+} ions (r = 0.645 Å). This substitution induces strains and disorders in the lattice structure. These changes limit the crystallization of material particles and hinder crystal growth. Similar results have also been reported for other spinel ferrite nanoparticles doped with various rare earth elements such as Gd-doped $CoFe_2O_4$ [20], Ce(Gd)-doped $NiFe_2O_4$ [29], and also for Eu-doped $CoFe_2O_4$ nanoparticles synthesized by hydrothermal method [30] and sonochemical technique [31].

Fig. 4 shows the EDX spectra of pure $CoFe_2O_4$ and $CoFe_{1.95}Eu_{0.05}O_4$ nanoparticles measured at room temperature. It is clear that for the x = 0 sample, only peaks of the elements Co, Fe, and O are observed. As for the Eu-doped $CoFe_2O_4$ sample (x = 0.05), in addition to the peaks of Co, Fe and O, peaks of the element Eu also appear. To accurately determine the content of elements in $CoFe_{2-x}Eu_xO_4$ samples (x = 0 and 0.05), EDXS analysis was recorded at 3 different positions in the sample. EDXS quantitative data showed that the ratios of Co/Fe/Eu/O elements for all samples were consistent with their ratios in the expected formula. This shows the high

Table 2. Refined structural parameters and crystallite size of $CoFe_{2-x}Eu_xO_4$ samples

Sample	D_{hkl}, nm	a, Å	V, Å^3
$CoFe_2O_4$	15.30	8.3554	583.31
$CoFe_{1.975}Eu_{0.025}O_4$	29.87	8.3449	581.12
$CoFe_{1.95}Eu_{0.05}O_4$	28.46	8.3405	580.20
$CoFe_{1.925}Eu_{0.075}O_4$	27.82	8.3366	579.38
$CoFe_{1.9}Eu_{0.1}O_4$	27.17	8.3215	576.24

purity of the synthesized $CoFe_{2-x}Eu_xO_4$ spinel nanoparticles.

To determine the morphology and grain size of the material synthesized, FE-SEM images of $CoFe_{2-x}Eu_xO_4$ samples (with x = 0 and 0.05) are shown in Fig. 5.

The particles have relatively uniform morphology with particle size of approximately 20–40 nm. Fig. 5 also shows that doping Eu^{3+} ion into the cobalt ferrite crystal lattice has an unclear effect on the morphology and size of the synthesized $CoFe_{2-x}Eu_xO_4$ nanoparticles. However, it is evident that both the pure doped sample have agglomeration between nanoparticles. Such agglomeration can be ascribed to the strong magnetic interactions between the particles, leading to mutual magnetization induction. Similar phenomenon was also observed in other spinel ferrites synthesized by different wet chemical methods [12, 15, 20, 28, 30, 32].

The optical properties of $CoFe_{2-x}Eu_xO_4$ nanoparticles (x = 0, 0.025, 0.05, 0.075, and 0.1) were determined through UV-Vis measurements in the wavelength range from 200 to 800 nm, corresponding to photon energy of 1.55 eV to 6.2 eV (Fig. 6). The optical band gaps (E_g, eV) of $CoFe_{2-x}Eu_xO_4$ nanoparticles were calculated using Tauc equation that correlates the absorption coefficient and E_g as below [11, 25, 28, 31]:

$$Ah\nu = \sqrt{\alpha(h\nu - E_g)}, \quad (5)$$

where A is the optical absorption coefficient, $h\nu$ is the photon energy, E_g is the direct band gap and α is a constant.

Fig. 6a shows that europium-doped cobalt ferrite nanoparticles exhibit strong optical absorption not only in the ultarviolet (λ = 200–400 nm) but also in visible light regions (λ = 400–800 nm). Particularly, the maximum absorption is observed in the wavelength range of 350–700 nm.

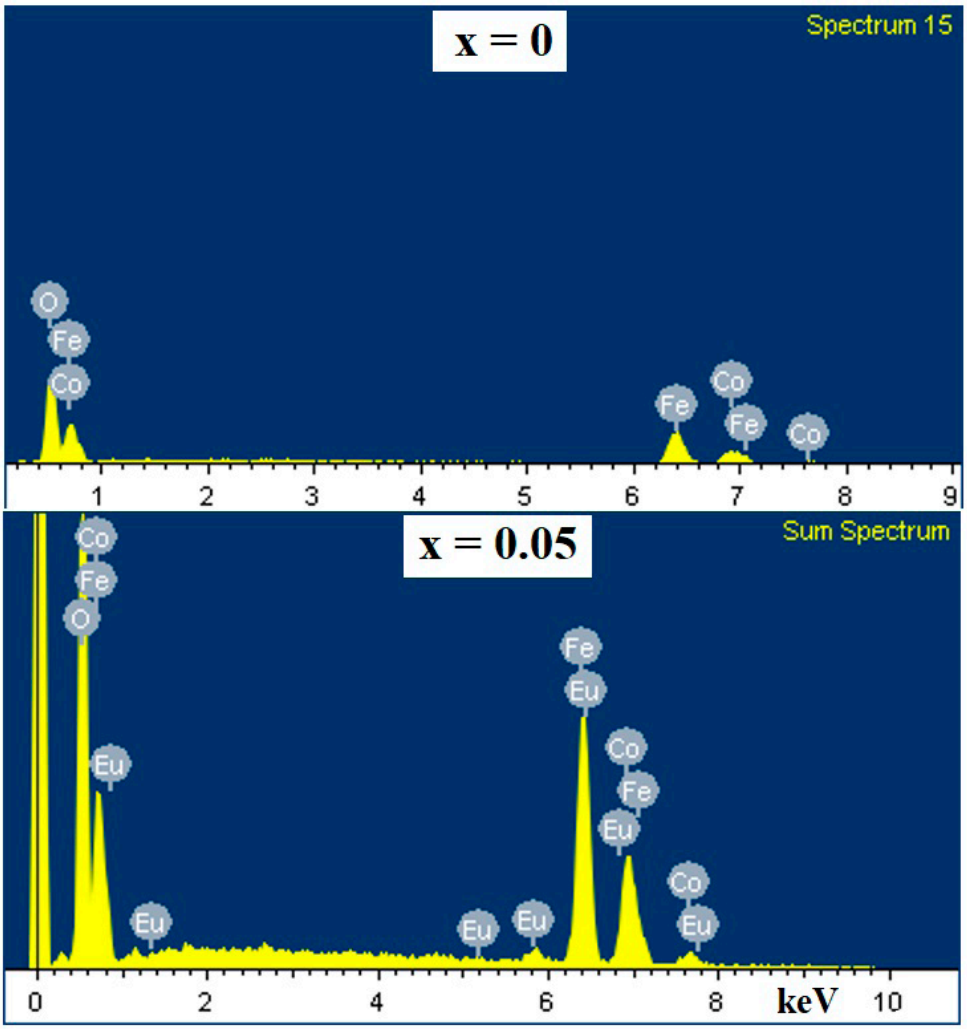

Fig. 4. Energy-dispersive X-ray spectroscopy (EDXS) spectra of pure $CoFe_2O_4$ (x = 0) and $CoFe_{1.95}Eu_{0.05}O_4$ (x = 0.05) nanoparticles

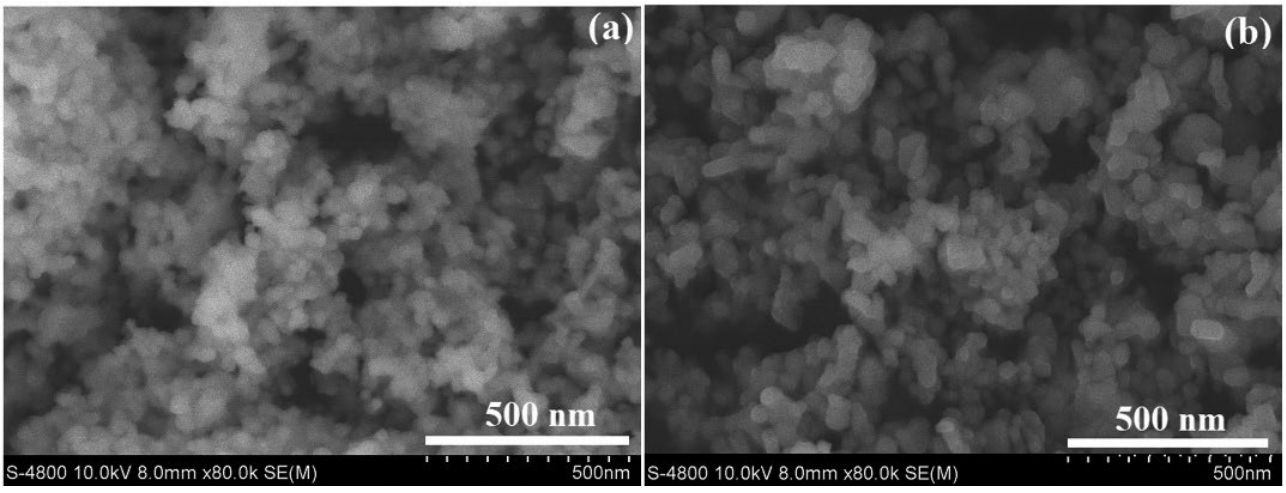

Fig. 5. Field emission scanning electron microscopy (FE-SEM) images of pure $CoFe_2O_4$ (a) and $CoFe_{1.95}Eu_{0.05}O_4$ (b) nanoparticles

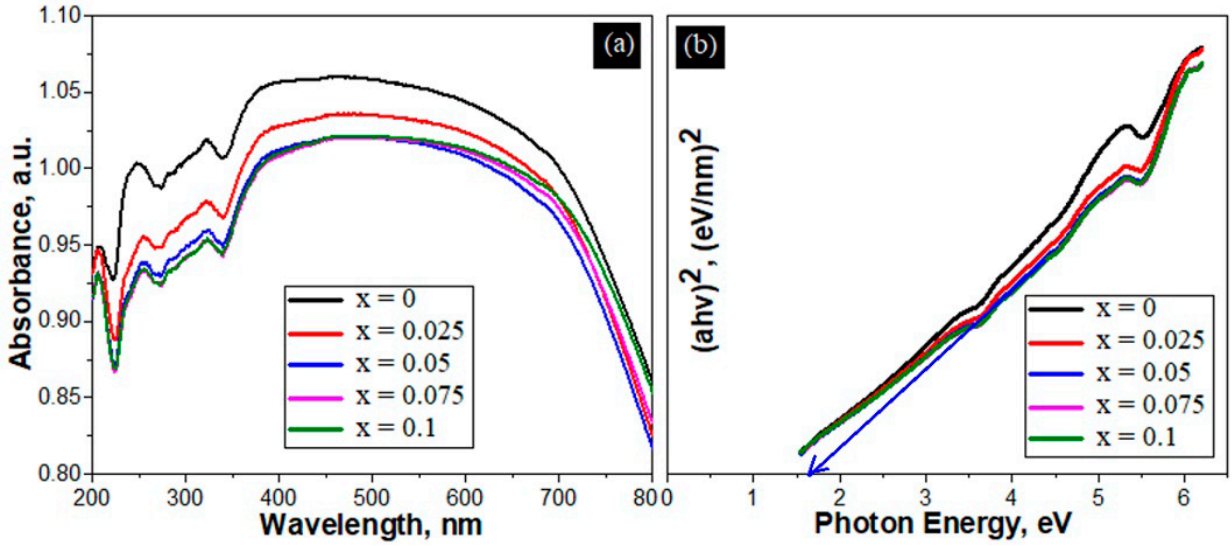

Fig. 6. (a) Room-temperature optical absorbance spectra of the $CoFe_{2-x}Eu_xO_4$ samples and (b) Plot of $(\alpha hv)^2$ as a function of photon energy for $CoFe_{2-x}Eu_xO_4$ nanoparticles

The absorption tends to decrease with increasing Eu^{3+} ion content, which also means that the band gap energy value (E_g) changes in the opposite trend (Fig. 6b and Table 3). The value of E_g increases from 1.37 eV to 1.55 eV corresponding to the value of x increasing from 0 to 0.1.

The increase of band gap energy values with increasing doping element content were also reported for other spinel cobalt ferrites systems such as $CoFe_{2-x}Y_xO_4$ ($x = 0 \rightarrow 0.04$, $E_g = 2.30 \rightarrow 2.58$ eV) synthesized by the urea-fueled combustion method [11] or $CoFe_{2-x}Eu_xO_4$ ($x = 0 \rightarrow 0.1$, $E_g = 1.34 \rightarrow 1.56$ eV) synthesized by sonochemical technique [31]. With strong optical absorption in wavelength range of 350–700 nm and semiconductor-like band gap energy values

Table 3. Optical and magnetic parameters of $CoFe_{2-x}Eu_xO_4$ nanoparticles at RT in this study and that from the published literature as a comparison

Sample	E_g, eV	H_c, Oe	M_r, emu·$^{-1}$	M_s, emu·g^{-1}	Ref.
$CoFe_2O_4$	1.37	962.96	32.97	72.08	In this work
$CoFe_{1.975}Eu_{0.025}O_4$	1.45	983.75	33.83	71.74	
$CoFe_{1.95}Eu_{0.05}O_4$	1.50	1029.67	34.20	70.05	
$CoFe_{1.925}Eu_{0.075}O_4$	1.53	1121.38	37.37	65.22	
$CoFe_{1.9}Eu_{0.1}O_4$	1.55	885.46	29.62	61.74	
$CoFe_2O_4$	–	120	9	41.2	[7]
$CoFe_2O_4$	–	495.72	23.34	67.37	[8]
$CoFe_2O_4$	–	762.04	27.83	61.80	[15]
$CoFe_2O_4$	–	575	21.2	87.56	[20]
$CoFe_2O_4$	–	880	27.7	79.5	[30]
$CoFe_2O_4$	2.30	1100	28	69	[11]
$CoFe_{1.995}Y_{0.005}O_4$	2.32	1318	27	63	
$CoFe_{1.99}Y_{0.01}O_4$	2.34	1520	26	62	
$CoFe_{1.98}Y_{0.02}O_4$	2.42	1676	20	50	
$CoFe_{1.97}Y_{0.03}O_4$	2.45	1804	19	49	
$CoFe_{1.96}Y_{0.04}O_4$	2.58	1900	12	33	

(E_g = 1.37–1.55 eV), the synthesized $CoFe_{2-x}Eu_xO_4$ nanoparticles can be applied as photocatalytic materials for the decomposition of dyes, phenol, nitrophenol, methyl orange, or methylene blue [5, 11, 13, 32].

Fig. 8a shows the *M*–*H* loops of $CoFe_{2-x}Eu_xO_4$ ferrite nanosystems with x = 0, 0.025, 0.05, 0.075, and 0.1 at room temperature (300 K) under applied magnetic field up to 15 kOe. The observed remanent magnetization (M_r) and coercivity (H_c) in all hysteresis loops indicate that all samples are hard ferrites at room temperature [34]. All three magnetic parameters (M_r, H_c, and M_s) of $CoFe_{2-x}Eu_xO_4$ nanoparticles vary with the Eu^{3+} ion content (Table 3). Specifically, H_c increases from 962.96 to 1121.38 Oe, M_r increases from 32.97 to 37.37 emu·g^{-1}, while M_s decreases from 72.08 to 61.74 emu·g^{-1}. The increase in H_c and M_r values with increasing content of doping elements (Eu^{3+} ion) is attributed to enhanced crystal anisotropy [34, 35]. Meanwhile, partial replacement of Fe^{3+} ions at octahedral sites by Eu^{3+} ions reduces the magnetization on the Fe^{3+} sites (B-sites), thereby reducing the total magnetization of the Eu-doped $CoFe_2O_4$ nanoparticles. Similar trend was also reported for the Y^{3+} doped spinel cobalt ferrites [11]. In general, all three values H_c, M_r, and M_s of $CoFe_{2-x}Eu_xO_4$ nanoparticles are larger than those reported for pure $CoFe_2O_4$ nanoparticles synthesized using different methods [7, 8, 15, 20, 30], with H_c and M_s are also larger than those of Y-doped $CoFe_2O_4$ nanoparticles [11] (Table 3).

Another noteworthy observation is that the synthesized $CoFe_{2-x}Eu_xO_4$ nanoparticles are strongly attracted by rare earth magnets. This, combined this with the semiconductor bandgap energy value, suggests that the synthesized Eu-doped $CoFe_2O_4$ nanoparticles can be used as photocatalytic materials under the influence of sunlight with easy recovery and reuse by rare earth magnets.

4. Conclusions

Undoped and Eu-doped $CoFe_2O_4$ nanoparticles were successfully prepared by the simple co-precipitation method with 5% NaOH as a precipitant. Eu^{3+} ion doping at the Fe^{3+} site in spinel cobalt affects not only the structural parameters (D_{hkl} and *a*) but also their magneto-optical properties. The FE-SEM images confirms the nanostructure character of the $CoFe_{2-x}Eu_xO_4$ samples with particle sizes ranging from 20 to 40 nm. When the Eu^{3+} ion doping content increased, the E_g (1.37–1.55 eV), M_r (32.97–37.37), and H_c (962.96–1121.38 Oe) increased, while the M_s (72.08–61.74 emu·g^{-1}) decreases. Synthesized $CoFe_{2-x}Eu_xO_4$ nanoparticles exhibit the behavior of a hard ferromagnetic material with a small band gap energy, making them suitable not only for photocatalytic applications but also for the production of permanent magnets, magnetic tapes, and magnetic recording materials in hard drives.

Contribution of the authors

Le N. K. N: Investigation, methodology & Software. Nguyen T. T. T.: Methodology, writing–original draft. Nguyen H. H.: Methodology &

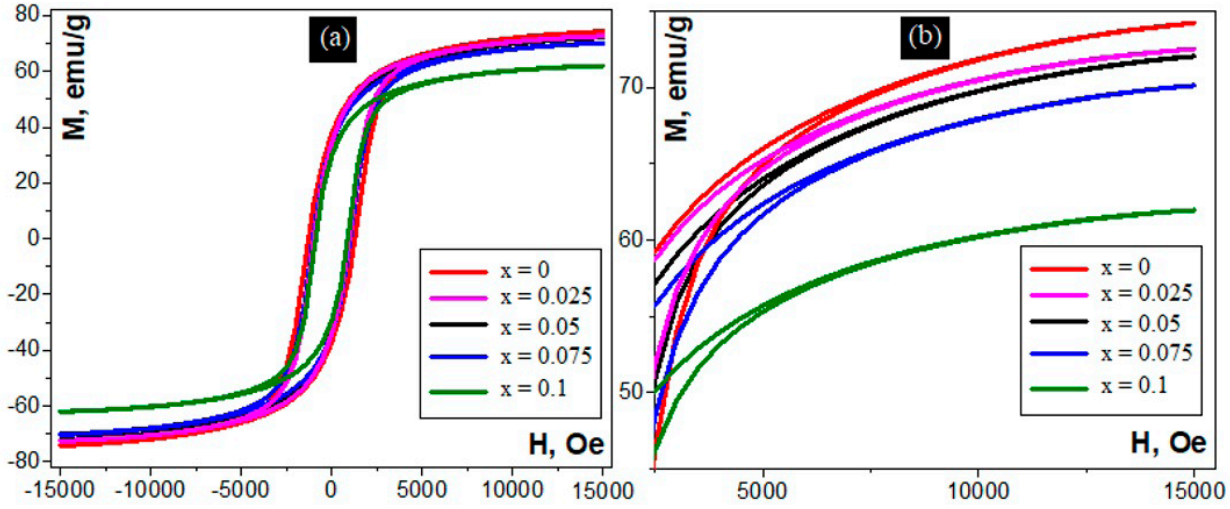

Fig. 7. *M*–*H* loops of $CoFe_{2-x}Eu_xO_4$ nanoparticles measured at room temperature

Software. Tran D. T.: Validation, Supervision & writing–original draft. Vu T. N. A.: Investigation, methodology & Formal analysis. Nguyen A. T.: Investigation, Data curation, Writing–review and editing. All authors have read and agreed to the published version of the manuscript.

Data availability statement

The data that support the findings of this study are available from the corresponding author upon reasonable request.

Conflict of interest

The authors maintain that they have no conflict of interest to be described in this communication.

References

1. Kebede K. K., Msagati T. A. M., Mamba B. B. Ferrite nanoparticles: synthesis, characterization and applications in electronic device. *Materials Science and Engineering: B*. 2017;215: 37–55. https://doi.org/10.1016/j.mseb.2016.11.002

2. Tomina E. V., Sladkopevtsev B. V., Nguyen A. T., Vo Q. M. Nanocrystalline ferrites with spinel structure for various functional applications. *Inorganic Materials*. 2023;59: 1363–1385. https://doi.org/10.1134/S0020168523130010

3. Zhang F., Wei C., Wu K., Zhou H., Hu Y., Preis S. Mechanistic evaluation of ferrite AFe_2O_4 (A = Co, Ni, Cu, and Zn) catalytic performance in oxalic acid ozonation. *Applied Catalysis A: Genenal*. 2017;547: 60–68. https://doi.org/10.1016/j.apcata.2017.08.025

4. Ivashenko D. V., Urbanovich D. A., Palyn I. Y., Bushinsky M. V., Trukhanov A. V., Pankov V. V. Synthesis dispersed powders of CoZn ferrites for microwave absorption. *Condensed Matter and Interphases*. 2023;25: 37–46. https://doi.org/10.17308/kcmf.2023.25/10646

5. Kefeni K. K., Mamba B. B. Photocatalytic application of spinel ferrite nanoparticles and nanocomposites in wastewater treatment: review. *Sustainable Materials and Technology*. 2020;23: e00140. https://doi.org/10.1016/j.susmat.2019.e00140

6. Wang L., Li J., Wang Y., Zhao L., Jiang Q. Adsorption capability for congo red on nanocrystalline MFe_2O_4 (M = Mn, Fe, Co, Ni) spinel ferrites. *Chemical Engineering Journal*. 2012;181: 72–79. https://doi.org/10.1016/j.cej.2011.10.088

7. Jain R., Kumar S., Meena S. K. Precipitating agent (NaOH and NH_4OH) dependent magnetic properties of cobalt ferrite nanoparticles. *AIP Advances*. 2022;12: 095109. https://doi.org/10.1063/5.0098157

8. Ngo T. P. H., Le T. K. Polyethylene glycol-assisted sol-gel synthesis of magnetic $CoFe_2O_4$ powders as photo-Fenton catalysts in the presence of oxalic acid. *Journal of Sol-Gel Science and Technology*. 2018;88: 211–219. https://doi.org/10.1007/s10971-018-4783-y

9. Nguyen A. T., Nguyen T. D., Mittova V. O., Berezhnaya M. V., Mittova I. Ya. Phase composition and magnetic properties of $Ni_{1-x}Co_xFe_2O_4$ nanocrystals with spinel structure synthesized by co-precipitation method. *Nanosystems: Physics, Chemistry, Mathematics*. 2017;8: 371–377. https://doi.org/10.17586/2220-8054-2017-8-3-371-377

10. Maaz K., Khalid W., Mumtaz A., Hasanain S. K., Liu J., Duan J. L. Magnetic characterization of $Co_{1-x}Ni_xFe_2O_4$ nanoparticles prepared by co-precipitation route. *Physical E: Low-dimensional Systems and Nanostructures*. 2009;41: 593–599. https://doi.org/10.1016/j.physe.2008.10.009

11. Alves T. E. P., Pessoni H. V. S., Franco Jr. A. The effect of Y^{3+} substitution on the structural, optical band-gap, and magnetic properties of cobalt ferrite nanoparticles. *Physical Chemistry Chemical Physics*. 2017;25: 16395–16405. https://doi.org/10.1039/C7CP02167D

12. Tomina E. V., Kurkin N. A., Doroshenko A. V. Synthesis of nanoparticulate cobalt ferrite and its catalytic properties for Fenton-like processes. *Inorganic Materials*. 2022;58: 727–732. https://doi.org/10.31857/S0002337X22070132

13. Thomas J., Thomas N., Girgsdies F., M. Beherns, ... Sebastiane V. Synthesis of cobalt ferrite nanoparticles by constant pH co-precipitation and their high catalytic activity in CO oxidation. *New Journal of Chemistry*. 2017;41: 7356–7363. https://doi.org/10.1039/c7nj00558j

14. Sumathi S., Lakshmipriya V. Structural, magnetic, electrical and catalytic activity of copper and bismuth co-substituted cobalt ferrite nanoparticles. *Journal of Materials Science: Materials in Electronics*. 2017;28: 2795–2802. https://doi.org/10.1007/s10854-016-5860-z

15. Nguyen T. T. L., Nguyen T. H. L., Nguyen T. T. H., ... Tran T. V. $CoFe_2O_4$ nanomaterials: effect of annealing temperature on characterization, magnetic, photocatalytic, and photo-Fenton properties. *Processes*. 2019;7: 885. https://doi.org/10.3390/pr7120885

16. Petrova E., Kotsikau D., Pankov V., Fahmi A. Influence of synthesis methods on structural and magnetic characteristics of Mg–Zn-ferrite nanopowders. *Journal of Magnetism and Magnetic Materials*. 2019;473: 85–91. https://doi.org/10.1016/j.jmmm.2018.09.128

17. Hoang B. K., Mittova V. O., Nguyen A. T., Pham T. H. D. Structural and magnetic properties of Ho-doped $CuFe_2O_4$ nanoparticles prepared by a simple co-precipitation method. *Condensed Matter and Interphases*. 2022;24: 109–115. https://doi.org/10.17308/kcmf.2022.24/9061

18. Patankar K. K., Jadhav P. S., Devkar J., Ghone D. M., Kaushik S. D. Synthesis and characterization of $CoFe_{2-x}Y_xO_4$ (x = 0.05 – 0.2) by auto combustion method. *AIP Conference Proceedings*. 2017;1832: 050172. https://doi.org/10.1063/1.4980405

19. Gingasu D., Mindru I., Ianculescu A.-C., ... Chifiriuc M. C. Chifiriuc, soft chemistry synthesis and characterization of $CoFe_{1.8}Re_{0.2}O_4$ (R = Tb, Er) ferrite. *Magnetochemistry*. 2022;8: 1–15. https://doi.org/10.3390/magnetochemistry8020012

20. Zhao X., Wang W., Zhang Y., Wu S., Li F., Liu P. Synthesis and characterization of gadolinium doped cobalt ferrite nanoparticles with enhanced adsorption capability for Congo Red. *Chemical Engineering Journal*. 2014;250: 164–174. https://doi.org/10.1016/j.cej.2014.03.113

21. Boddolla S., Ravinder D. Eu^{3+} doped $CoFe_2O_4$ nanoparticles with XRD and FTIR analysis. *Journal for Research in Applied Sciences and Biotechnology*. 2024;3: 135–138. https://doi.org/10.55544/jrasb.3.2.23

22. Franco A. Jr., Pessoni H. V. S., Alves T. E. P. Enhanced dielectric permittivity on yttrium doped cobalt ferrite nanoparticles. *Materials Letters*. 2017;208: 115–117. https://doi.org/10.1016/j.matlet.2017.04.101

23. Basak M., Rahman M. L., Ahmed M. F., Biswas B., Sharmin N. Calcination effect on structural, morphology and magnetic properties of nano-sized $CoFe_2O_4$ developed by a simple co-precipitation technique. *Materials Chemistry and Physics*. 2021;264: 124442. https://doi.org/10.1016/j.matchemphys.2021.124442

24. Nguyen A. T., Nguyen T. T., Mittova V. O., ... Bui X. V. Structural, thermal, and magnetic properties of orthoferrite $EuFeO_3$ nanoparticles prepared by a simple co-precipitation method. *Journal of Materials Science: Materials in Electronic*. 2023;34: 1370. https://doi.org/10.1007/s10854-023-10779-y

25. Nguyen A. T., Cam T. S., Mittova V. O., ... Bui X. V. Influence of synthesis conditions on the crystal structure, optical and magnetic properties of *o*-$EuFeO_3$ nanoparticles. *Coatings*. 2023;13: 1082. https://doi.org/10.3390/coatings13061082

26. Tran D. T., Nguyen H. C. H., Le T. T. T., Nguyen A. T. Effect of annealing temperature and precipitation agent on the structure, optical and magnetic characteristics of dysprosium orthoferrite nanoparticles. *Materials Today Commnunications*. 2024;40: 109733. https://doi.org/10.1016/j.mtcomm.2024.109733

27. Housecroft C. E.; Sharpe A. G. *Inorganic Chemistry*, 2nd ed. NJ, USA: Pearson, Prentice Hall, Upper Saddle River; 2005. 950 p.

28. Tien N. A., Mittova V. O., Sladkopevtsev B. V., ... Vuong B. X. Structural, optical and magnetic properties of Y-doped $NiFe_2O_4$ nanoparticles prepared by simple co-precipitation method. *Solid State Sciences*. 2023;138: 107149. https://doi.org/10.1016/j.solidstatesciences.2023.107149

29. Dixit G., Singh J. P., Srivastava R. C., Agrawal H. M. Magnetic resonance study of Ce and Gd doped $NiFe_2O_4$ nanoparticles. *Journal of Magnetism and Magnetic Materials*. 2012;324: 479–483. https://doi.org/10.1016/j.jmmm.2011.08.027

30. Mohamed W. S., Abu-Dief A. M. Impact of rare earth europium (Re-Eu^{3+}) ions substitution on microstructural, optical and magnetic properties of $CoFe_{2-x}Eu_xO_4$ nanosystems. *Ceramics International*. 2020;46: 16196–16209. https://doi.org/10.1016/j.ceramint.2020.03.175

31. Almessiere M. A., Slimani Y., Korkmaz A. D., ... Ozcelik B. Sonochemical synthesis of Eu^{3+} substituted $CoFe_2O_4$ nanoparticles and their structural, optical and magnetic properties. *Ultarsonics Sonochemistry*. 2019;58: 104621. https://doi.org/10.1016/j.ultsonch.2019.104621

32. Chung N. T. K., Tien N. A. Structural, optical and magnetic properties of Y-doped $CoFe_2O_4$ nanoparticles prepared by a simple co-precipitation method. *Journal of Materials Science: Materials in Electronic*. 2023;34: 448. https://doi.org/10.1007/s10854-023-09914-6

33. Ahmadi H., Shokrollah N., Aghaei S., ... Tightiz N. Nanocrystalline $CuFe_{2-x}Sm_xO_4$: synthesis, characterization and its photocatalytic degradation of methyl orange. *Journal of Materials Science: Materials in Electronic*. 2016;27: 4689–4693. https://doi.org/10.1007/s10854-016-4347-2

34. Cullity B. D., Graham C. D. *Introduction to Magnetic* Materials, 2nd ed. Canada: John Wiley & Sons, Inc., Publication; 2009. http://doi.org/10.1002/9780470386323

35. Moriya Y. New mechanism of anisotropic superexchange interaction. *Physical Review Letters*. 1960;4: 228–230. https://doi. org/10.1103/PhysRevLett.4.228

Information about the authors

Khanh Nhu Le Ngoc, 3nd year student, Faculty of Chemistry, Ho Chi Minh City University of Education (Ho Chi Minh City, Vietnam).
nhukhanhngoc1010@gmail.com

Thu Trang Nguyen Thi, PhD in Chemistry, Faculty of Chemistry, Ho Chi Minh City University of Education (Ho Chi Minh City, Vietnam).
https://orcid.org/0009-0009-6825-4625
thutrang@hcmue.edu.vn

Hoang Huy Nguyen, 1st postgraduate student, Inorganic Chemistry Department, Faculty of Chemistry, Ho Chi Minh City University of Education (Ho Chi Minh City, Vietnam).
https://orcid.org/0009-0001-7209-2114
huynh@phd.hcmue.edu.vn

Dinh Trinh Tran, PhD in Chemistry, Associate Professor, VNU Key Laboratory of Advanced Materials for Green Growth, University of Science, Vietnam National University (Hanoi, Vietnam).
https://orcid.org/0000-0001-9936-1823
trinhtd@vnu.edu.vn

Ngoc Anh Vu Thi, PhD in Chemistry, Ton Duc Thang University (Ho Chi Minh City, Vietnam).
https://orcid.org/0000-0002-0510-1762
vuthingocanh@tdtu.edu.vn

Anh Tien Nguyen, PhD in Chemistry, Associate Professor, Head of the Inorganic Chemistry Department, Ho Chi Minh City University of Education (Ho Chi Minh City, Vietnam).
https://orcid.org/0000-0003-3919-8571
tienna@hcmue.edu.vn

Received February 27, 2025; approved after reviewing March 19, 2025; accepted for publication March 25, 2025; published online December 25, 2025.